



Issues concerning roughness on wind turbine blades

Ece Sagol^{a,*}, Marcelo Reggio^a, Adrian Ilinca^b

^a Polytechnique Montréal, 2500 Chemin de Polytechnique, Montréal, QC, Canada H3T 1J4

^b Université du Québec à Rimouski (UQAR), 300, allée des Ursulines, Rimouski, QC, Canada G5L 3A1

ARTICLE INFO

Article history:

Received 11 September 2012

Received in revised form

13 February 2013

Accepted 18 February 2013

Available online 9 April 2013

Keywords:

Wind turbine

Wind turbine power reduction

Surface roughness

Ice accumulation

Dust accumulation

Wind turbine icing

Wind turbine contamination

ABSTRACT

This paper reviews the effects of surface roughness, accreted on wind turbine blades, on the flow field and power generation. Contamination agents, like dust, dirt, ice, and even insects accumulate on the blades and generate roughness to varying degrees. These roughness elements, depending on their size, location, and density, may disturb the flow field and reduce the power produced by the machine. A review of papers addressing similar flow patterns is provided, along with an analysis of the ability of numerical algorithms to correctly predict the power performance and the flow characteristics in the presence of surface irregularities. Finally, solutions are given to mitigate the effects of roughness on power production.

© 2013 Elsevier Ltd. All rights reserved.

Contents

| | |
|---|-----|
| 1. Introduction | 514 |
| 2. Surface roughness and its sources | 515 |
| 2.1. Dust accumulation | 515 |
| 2.2. Insect contamination | 515 |
| 2.3. Ice accumulation | 516 |
| 2.4. Other roughness sources | 516 |
| 2.5. Characterization of roughness | 516 |
| 3. Effects of roughness on flow field | 516 |
| 4. Effects of roughness on performance | 518 |
| 5. Numerical efforts for modeling roughness | 521 |
| 6. Solutions to the roughness problem | 522 |
| 6.1. Specially designed airfoils | 522 |
| 6.2. External solutions | 523 |
| 7. Concluding remarks | 524 |
| References | 525 |

1. Introduction

The world's demand for energy is increasing due to rapidly growing population and industrial production. Although fossil fuels are still the primary and the most widely used energy source,

problems related to their contribution to global warming and finding new supplies are prompting us to seek cleaner and more sustainable alternatives, i.e. renewable energy. Prominent among those alternatives is wind energy, which is widely available at a competitive cost.

Wind turbines can be exposed to dramatically different operational conditions, from icy, arctic-type environments to deserts with sand storms, and there are contaminants in all of them, like dust, dirt, ice, and even insects, that affect the surfaces of a wind turbine blade. These contaminants generate irregularities on this once

* Corresponding author. Tel.: +1 514 739 8539.

E-mail addresses: ece.sagol@polymtl.ca, ecesaragol@gmail.com (E. Sagol).

smooth surface, perturbing the flow field around the blade. The affected wind turbines produce less energy than expected, which leads to an economic problem beyond the initial engineering challenge.

This paper is structured in several parts to explain the issues related to the effects of surface roughness on wind turbine blade aerodynamics. In the first part (Section 2), the circumstances leading to surface contamination are described, with a brief description of the physical characteristics of roughness. In the second part (Sections 3 and 4), the effect of surface roughness on blade aerodynamics and turbine performance is analyzed, emphasizing the experimental results available in the literature. Then, numerical algorithms that simulate the presence of roughness are examined, with special attention given to turbulence modeling (Section 5). Finally, solutions to reduce the impact of roughness are reviewed, and the design of airfoils that are ‘impervious’ to roughness is considered (Section 6).

2. Surface roughness and its sources

Wind turbines are unavoidably exposed to the environmental conditions that prevail in the location where they are erected. The environment may be harsh, or it may contain particles, and even insects, that erode or contaminate the blade surfaces. Of these contaminants, dust, ice, and insects are the agents known to increase the roughness of the blade the most [1–3]. Fig. 1 shows examples of contamination by these agents and of the effects of erosion.

2.1. Dust accumulation

Small particles of dust, dirt, and sand can be transported by the wind to the height of the wind turbine rotor. As these particles hit the rotor blade, the smoothness of the surface is perturbed, especially at the leading edge, near the stagnation point. While dust contamination has not been extensively examined, a few studies have resulted in some key findings which explain the effects of dust roughness on wind turbine blades, and the relationship between power output, the duration of dust exposure, and grain size.

In the study by Khalfallah and Koliub [4], the effects of dust accumulation on a 300 kW pitch regulated wind turbine, over various operational periods, are examined. As expected, the dust accumulation pattern follows the blade profile, with the highest concentration of particles on the leading edge and the tip of the blade.

2.2. Insect contamination

Although there is no doubt about the possibility of insect contamination on wind turbine blades, the presence of insects was not considered a source of a significant power loss until recently. At wind farms in California [5,6], different power levels were detected in several wind turbines. In other words, the

turbines showed multiple power curves for the same wind speed. To find the source of this phenomenon, Corten and Veldkamp [5] developed several hypotheses, all of which have been examined experimentally. They validate the possibility of insect accretion, concluding that wind turbine blades are contaminated only at low speed winds in which insects can fly. At these speeds, power production is not significantly influenced by roughness. However, at high wind speeds, there is a remarkable decrease in power output due to surface roughness generated by insects. Moreover, according to this hypothesis, the contamination level also depends on the atmospheric conditions in which insects fly: above 10 °C, and when it is not raining. Very low temperature and low humidity also contribute to an insect-free environment [7]. In addition to atmospheric conditions, insect presence also depends on altitude, with a rapidly decreasing density from ground level to 500 ft [8]. The conditions for insect contamination are schematized in Fig. 2. The increase shown in the power curve is the result of the blades having been cleaned by rain.

To validate the hypothesis, two juxtaposed wind turbines were investigated experimentally at the same wind farm. The first turbine, a clean one, was subjected to natural contamination by insects, and an artificial surface roughness was applied to the second one. The power outputs of these turbines were periodically recorded during the experiment. Initially, the first one generated more power than the second. As the contamination level increased over time, the power level of first turbine decreased, and approached the power production of the second turbine. In other words, natural contamination generated a level of surface roughness equivalent to that of the second turbine. These results validate the hypothesis that insect accumulation, by increasing the roughness of the blade surface, leads to power reduction [5].

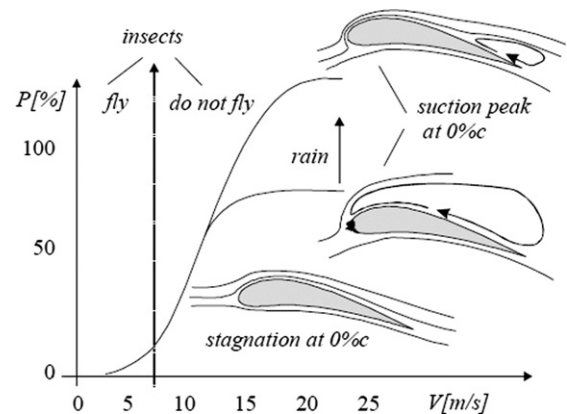


Fig. 2. Conditions for insect contamination [5].



Fig. 1. Rough surfaces of wind turbine blades caused by insects, ice, and erosion, respectively [1–3].

2.3. Ice accumulation

The influence of accreted ice has been extensively studied, both for airplanes and wind turbines, as the consequences and risks are considerable for the operation of these machines. Ice accumulates as super cooled water droplets present in clouds strike the solid surfaces and freeze on contact. The ice shapes that form on these machines and their effect on performance are schematized for different types of ice accretion in Fig. 3 [9]. The ice build-up on these structures is classified as glaze (horn) ice, rime (streamwise) ice, ridge ice, and ice roughness. Glaze ice is horn-shaped, and forms where a thin water layer covers a thicker ice layer. This horn shape originates from the runback water that does not freeze on impact, but after moving towards the trailing edge. Rime, or streamwise ice, contains ice layers that form at the intersection of water droplet streamlines and solid surfaces. As indicated in Fig. 3, rime ice has a less negative effect on the flow field, whereas glaze ice, because of its shape, has more. These two ice formations, because they occur the most frequently, are the types most often studied in the literature. Ridge ice forms as a single large obstacle on the suction side of the turbine, and causes a huge separation bubble, deforming the flow field more significantly than the other types of ice, as shown in Fig. 3. Finally, ice roughness refers to any type of icing at early stage in its formation, where water droplets are not able to form an ice layer, but can perturb the profile of the blade. Although ice roughness exists at the initial stage of any type of icing process, it can influence performance substantially, the extent of its effect depending on its height, concentration, and location. Ice roughness modifies the thickness of the boundary layer and the extent of its transitional characteristics, which depend on its height, location, and Reynolds number. Consequently, the corresponding aerodynamic characteristics, like lift and drag coefficients, are influenced as well. These phenomena are addressed in detail in the next sections.

2.4. Other roughness sources

In addition to contamination induced roughness, surface finishing and surface degradation due to erosion also contribute to roughness effects on wind turbine blades. As well, poor surface

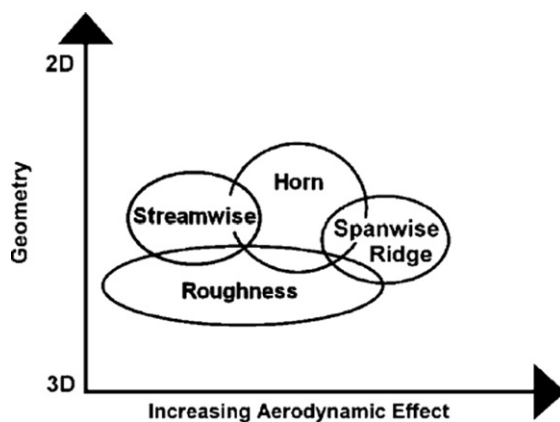


Fig. 3. Classification of ice accumulation types [9].

Table 1
Roughness values of surface finish applications (reproduced from [10]).

| Application process | Resulting surface roughness (μm) |
|---------------------|---|
| Roller | 55–80 |
| Roller+Sanding | 35–55 |
| Spraying | 10–23 |

finishing may cause power loss during operation. As a protective layer and to reduce the level of roughness, paint is applied to the blade surface. Pechlivanoglou [10] has published the resulting surface roughness for various painting processes—see Table 1. The technique of spraying generates minimal roughness on the surface; however, special care must be taken to prevent any particles from sticking to the surface during the process, as these would raise the surface roughness level.

2.5. Characterization of roughness

Whatever the source, dust, ice, or insects, roughness on a surface is characterized by its height, concentration, and location. Roughness height refers to the size of a single roughness element, or an average of multiple roughness elements, on a surface. Roughness size can be defined by its height from the surface for randomly shaped elements, and by its diameter for spherical elements. However, to compare several cases accurately, the roughness height, k , is non dimensionalized by the chord length, c , and represented as k/c . Consequently, for applications with similar Reynolds numbers, the aerodynamic characteristics can be compared based on the k/c value. Roughness density refers to how densely the roughness elements are distributed on the surface. The effects of various roughness configurations, namely densely and sparsely distributed elements, have been investigated in many studies. Finally, roughness location refers to the area where the roughness elements are present. As the contamination particles follow the streamwise flow, they tend to build up near the stagnation point, which is usually at the leading edge. The dependency of turbine performance on these parameters is explained in following sections.

3. Effects of roughness on flow field

From the fluid dynamics point of view, roughness can be defined as a surface extension of a body that penetrates into the viscous layer. These elements increase the interaction surface between fluid and solid, causing irregularities and disturbing flow field within the boundary layer. Consequently, momentum and energy transfer between the surface and the flow will increase, which will affect the aerodynamic performance of the airfoil.

According to the stability theory explained by Schlichting [11], there are small fluctuations in the flow quantities, which are velocity, pressure, density, and temperature. If these fluctuations are substantial enough to affect the mean flow quantities, a transitional period will occur, during which the flow will change its regime from laminar to turbulent. This transition is illustrated in Fig. 4.

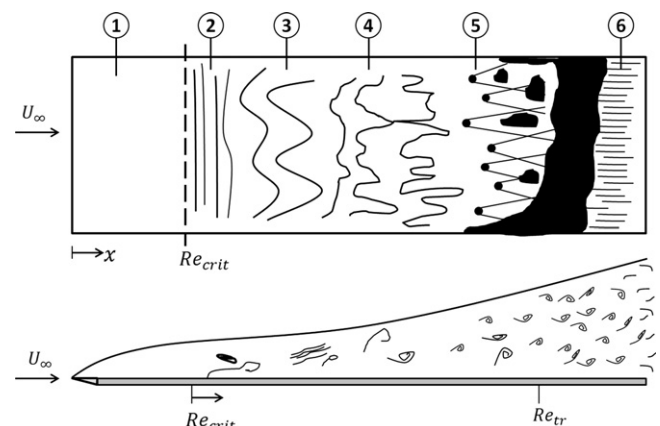


Fig. 4. Transition from laminar to turbulent flow [11].

As we can see from the figure, while the flow is laminar at the upstream point 1, it reaches a critical Reynolds number and the transition process starts. During the transition, from point 2 to point 6, various complex flow structures are formed. Depending on the characteristics of the flow and the surface, some of these stages could be bypassed or extended. Several studies [11–14] have shown that there are two important effects of surface roughness on the boundary layer transition: the transition point moves upstream on the wall, which implies an early transition and a prolonged period of transition. To validate these effects, Turner et al. [13] performed flow visualizations of boundary layers for both clean and rough surfaces. Although this study was intended to investigate roughness elements for turbomachine blades, it is also useful in helping to explain the flow behavior for rough and curved surfaces for Reynolds numbers of around 5×10^6 . As we can see in Fig. 5(a), a transition of the flow from laminar to turbulent was observed for the clean configuration, whereas only a turbulent boundary layer was observed for the rough configuration (Fig. 5(b)). It is clear that leading edge roughness provokes early transition of the boundary layer. Moreover, Laser Doppler Anemometer (LDA) measurements on the viscous layer of the clean and the rough configurations (graph in Fig. 5) shows that the turbulence intensity for the rough configuration is significantly higher near the wall, and, although not

illustrated here, the streamwise velocity gradient is less stable. This is to be expected, as the area of the turbulent boundary layer of the rough surface is larger in this case.

Kerho and Bragg [14] also examined the transition on a NACA 0012 airfoil for various Reynolds numbers, roughness locations (s), and roughness sizes. Results show that roughness elements cause a slower transition of the boundary layer, depending on roughness size and location, as well as Reynolds number. In Fig. 6, the lower Reynolds number flow does not seem to be significantly affected by the size of the roughness elements. Various studies [9–15] show that there is a critical Reynolds number under which flow field and performance are not affected by the presence of roughness elements. At higher Reynolds numbers, the effect of roughness becomes very significant, regardless of its size and location. The transitional area also increases relative to that of a clean configuration. The change in the size of the transitional area has direct effect on the aerodynamic coefficients (lift and drag), and is discussed in the following section.

Roughness elements also modify the level of turbulence intensity on the surface. Bragg et al. [9] presented an example of turbulence intensity increase for clean and rough NACA 0012 configurations for a Reynolds number of 1.25×10^6 . As shown in Fig. 7, roughness elements not only provoke early transition, but also contribute to higher turbulence intensity levels during the transition.

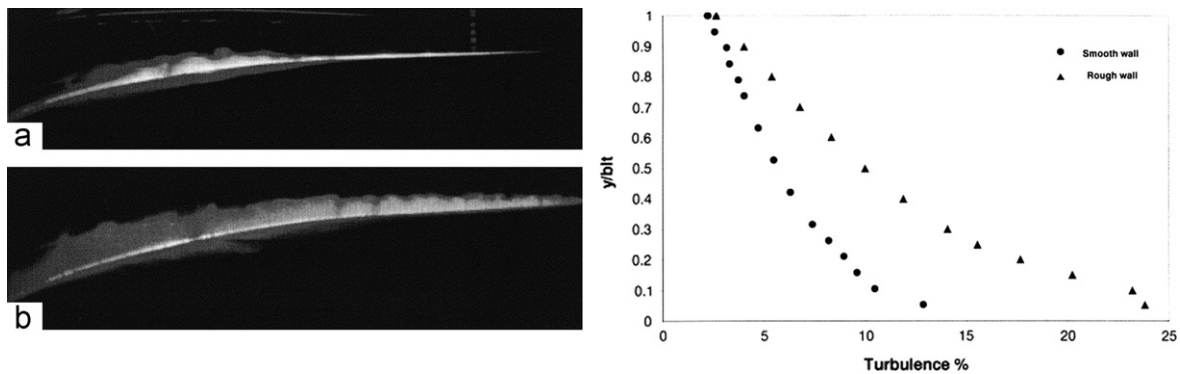


Fig. 5. Boundary layer transition and turbulence intensity: (a) on a smooth surface; and (b) on a rough surface [13].

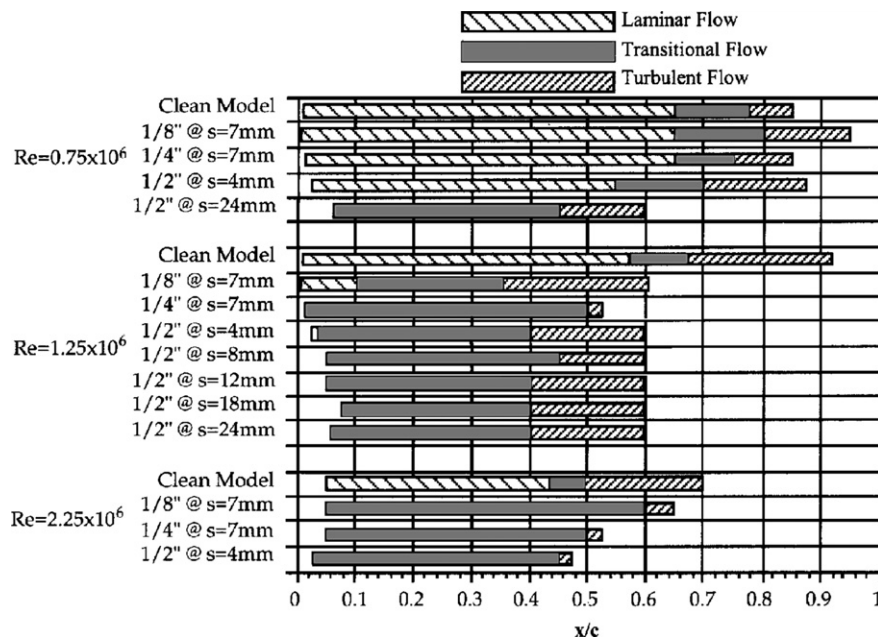


Fig. 6. Transition over the surface of a NACA 0012 for various Reynolds numbers [14].

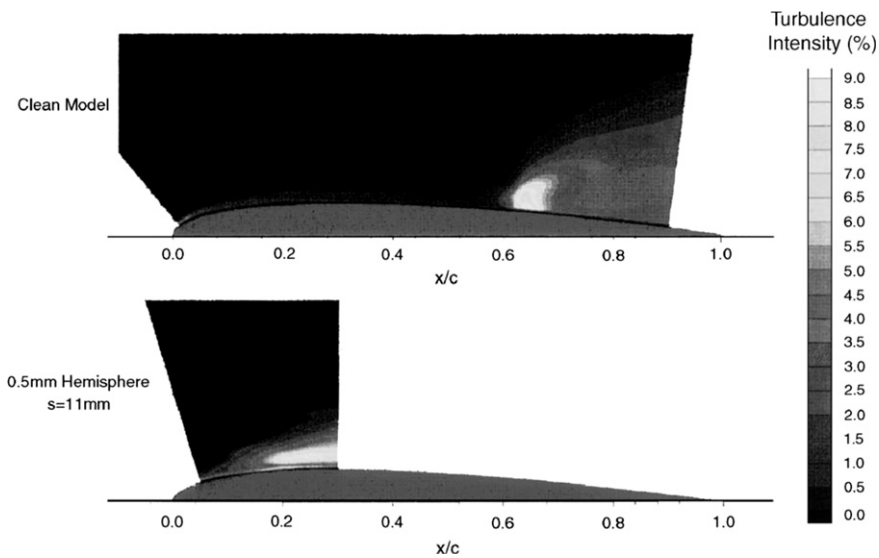


Fig. 7. Turbulence intensity level for a clean and a rough NACA 0012 [9].

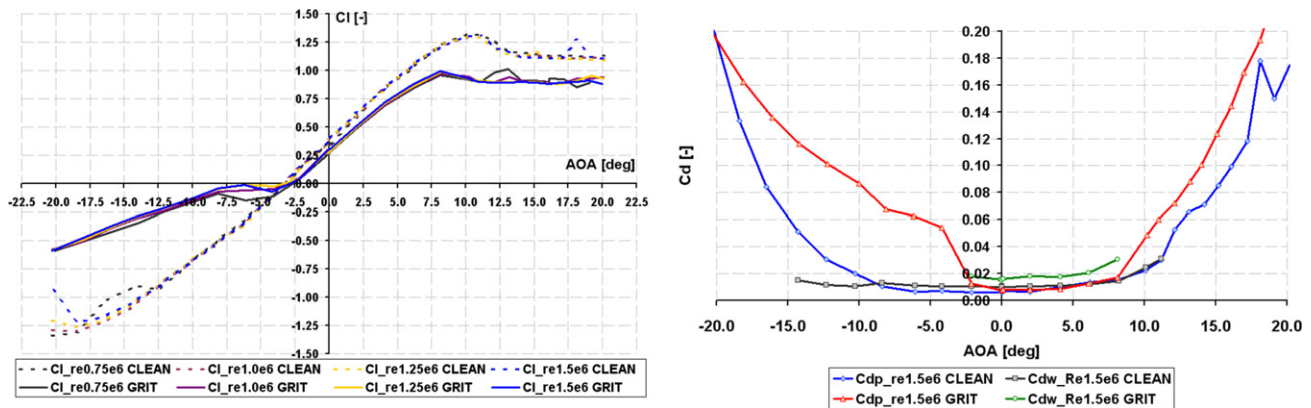


Fig. 8. Lift and drag coefficient curves for clean and rough configurations [15].

4. Effects of roughness on performance

As mentioned, roughness on a blade surface degrades wind turbine performance by decreasing the maximum lift coefficient and increasing the drag coefficient. To quantify the performance loss due to roughness, several researchers [4–8,15–19] have performed wind tunnel experiments and numerical simulations on wind turbine blades and airfoils. For the S814 airfoil, a molded insect pattern with a roughness size of $k/c=0.0019$ was applied to the model surface in a wind tunnel by Ferrer and Munduate [15]. Fig. 8 shows lift and drag coefficient curves for various angles of attack and Reynolds numbers. The lift coefficient decreases, especially for higher angles of attack, for both positive and negative values. The viscous drag increases with roughness, whereas the pressure drag is affected at higher angles of attack where separation takes place.

Although applying a molded pattern for the simulation of a rough surface may represent the real cases quite well, it is not practical in terms of cost and application time. For this reason, roughness on a surface is usually simulated using various contamination agents or strips, or other roughness elements. For example, Busch [12] proved that a roughness can be simulated by applying grit to the surface. Results of the simulations on a NACA 23-012 airfoil in a refrigerated wind tunnel are shown below in Fig. 9a and Fig. 9b. As seen, modeling with a 3D casting model and with grit roughness generally yield similar lift and drag

coefficients. It can be concluded that, although there is a bias in the drag coefficient at low angles of attack, applying grit can replace 3D casting to simulate roughness on a surface, and it is cheaper and more practical (Fig. 9).

In the paper by Freudenreich et al. [16], clean and rough configurations of a thick, state-of-the-art wind turbine blade are investigated experimentally and numerically. Three different roughness configurations are examined. A tripping wire 1 mm in diameter was applied to the suction side at $0.3c$; 0.4 mm and 0.6 mm zigzag tapes were applied to the suction side at $0.05c$ and $0.1c$, respectively; and, finally, 60 grain carborundum (Carborundum 60) was applied to the leading edge of the model, up to $0.07c$ of both the suction and pressure sides. The latter configuration has greater roughness density and a more realistic roughness distribution. The tripping wire caused an increase in both the lift and drag coefficients, which is more noticeable in the latter parameter. However, the overall lift-to-drag ratio decreased relative to that of the clean configuration. For the zigzag tape configurations, both the maximum lift coefficient and the lift-to-drag ratio decreased. A reduction in these quantities is associated with a reduction in the power production of the wind turbines. The configuration treated with Carborundum 60 represents the most realistic roughness model, as it is applied to the entire leading edge, whereas in the other configurations, it is applied to a section only. Results for this configuration show that the boundary layer goes into early transition at the leading edge.

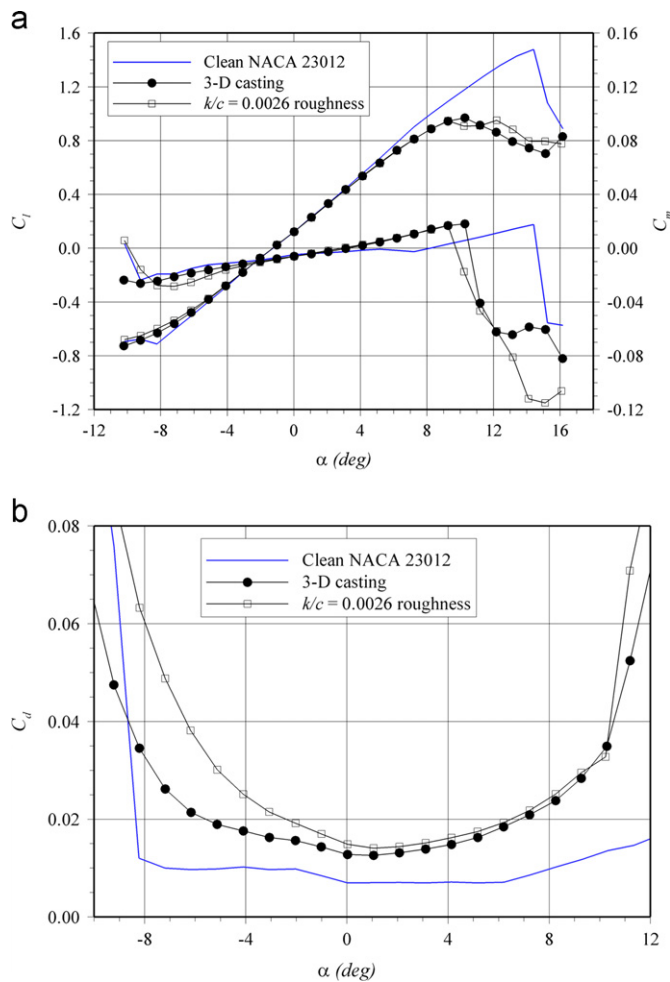


Fig. 9. (a) Lift; and (b) drag coefficient curves for clean surfaces and surfaces with roughness applied [12].

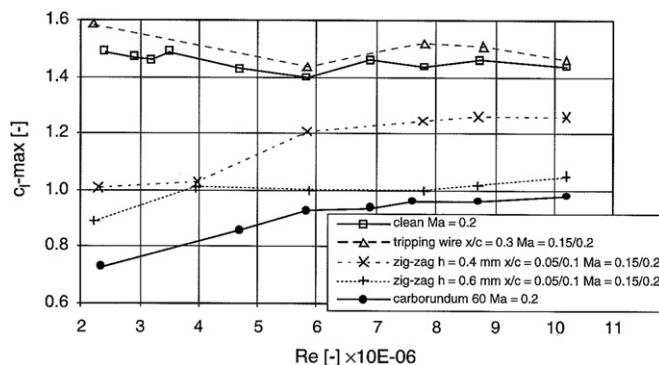


Fig. 10. Effect of various roughness configurations on a wind turbine blade [16].

Moreover, as the boundary layer thickens due to the roughness elements, drag increases and early stall is induced. For this configuration, the Reynolds number serves as a stabilizing factor on stall, as the boundary layer thickness decreases with an increasing Reynolds number. An overall comparison of these configurations in terms of lift-to-drag ratio is presented in Fig. 10, which shows that the maximum lift-to-drag ratio is yielded by Carborundum 60, which is around 40% of that of the clean configuration.

Results of another study that measured the lift and drag coefficients for clean and rough configurations of a NACA63-x18 airfoil are shown in Fig. 11(a) and (b) [17]. NACA standard

roughness was applied on the leading edge, up to 8% of the chord on the upper and lower surfaces. Comparing these configurations, it is clear that the maximum lift coefficient decreases by approximately 20%, whereas the drag coefficient almost doubles.

Li et al. [18] examined the effect of roughness size and density numerically on a DU 95-W-180 airfoil. Roughness heights ranging from 0.03 mm to 2 mm were applied to the numerical model. As we can see in Fig. 12, lift and drag coefficients are greatly influenced by roughness height. However, there is a point where these coefficients become insensitive to roughness height, which is called the critical roughness size in the literature. For this airfoil, the critical roughness height seems to be between 0.5 mm and 1 mm.

Similarly, Bragg et al. [9] discuss the effect of roughness location and height on the lift coefficient based on data they collected from various studies. Fig. 13, taken from this study, clearly shows that the maximum lift coefficient loss increases as the roughness size increases. However, the amount of the loss is highly dependent on the roughness location, which we discuss in the next section.

The location of roughness elements on the blade surface is also an important parameter that modifies machine performance. Gregory and O'Reilly [19] examine the effect of the roughness location on a NACA 0012 airfoil. A typical ice layer of 0.3 mm roughness height is investigated for both sparsely and densely populated roughness elements at Reynolds number 2.88×10^6 . These experiments show that, when the roughness elements are applied to the trailing edge up to arc length $0.5c$ of the airfoil, an increase in the drag coefficient and only a slight decrease in the lift coefficient are observed. Moreover, the maximum lift coefficient remains constant. Consequently, it can be concluded that trailing edge roughness has very little effect on airfoil performance. As the roughness distribution approaches the leading edge, the change in performance becomes significant: the maximum lift coefficient gradually decreases from 1.5 to 1.1, the lift coefficient decreases by about 40%, and the drag coefficient doubles at the leading edge. This study also examines the effect of roughness density on airfoil performance. The authors state that more densely populated roughness elements result in worse performance, compared to sparsely populated roughness elements in the same conditions. For airfoils with leading edge roughness and for those that are rough over their entire surface area, the maximum lift coefficient decreases and the drag coefficient increases significantly for all the operational angles of attack.

Ren and Ou [20,21] also analyze the effect of roughness location on a NACA 63-430 airfoil using numerical simulation. As seen in Fig. 14, they conclude that the first half of the upper surface, i.e. the leading edge section, is much more sensitive to roughness than the trailing edge section.

Timmer et al. [17] demonstrate the effect of “wrap around” roughness, where roughness elements are distributed over the entire surface area of a 64-4xx wind turbine airfoil. Tests were performed with wrap around roughness and leading edge roughness with NACA standard roughness elements. Results show that wrap around roughness decreases the maximum lift coefficient by about 20% and increases the drag coefficient by 50%, while leading edge roughness decreases the maximum lift coefficient by about 5% and increases the drag coefficient by about 20%.

Although the roughness period is not a direct characteristic of roughness elements, it is an important parameter for quantifying the effect of roughness on wind turbine performance. The longer the roughness period, the more contamination develops on a surface. This is why we can expect the multiple effects of increasing both roughness size and roughness density during longer roughness periods. Corten and Veldkamp [5] measured

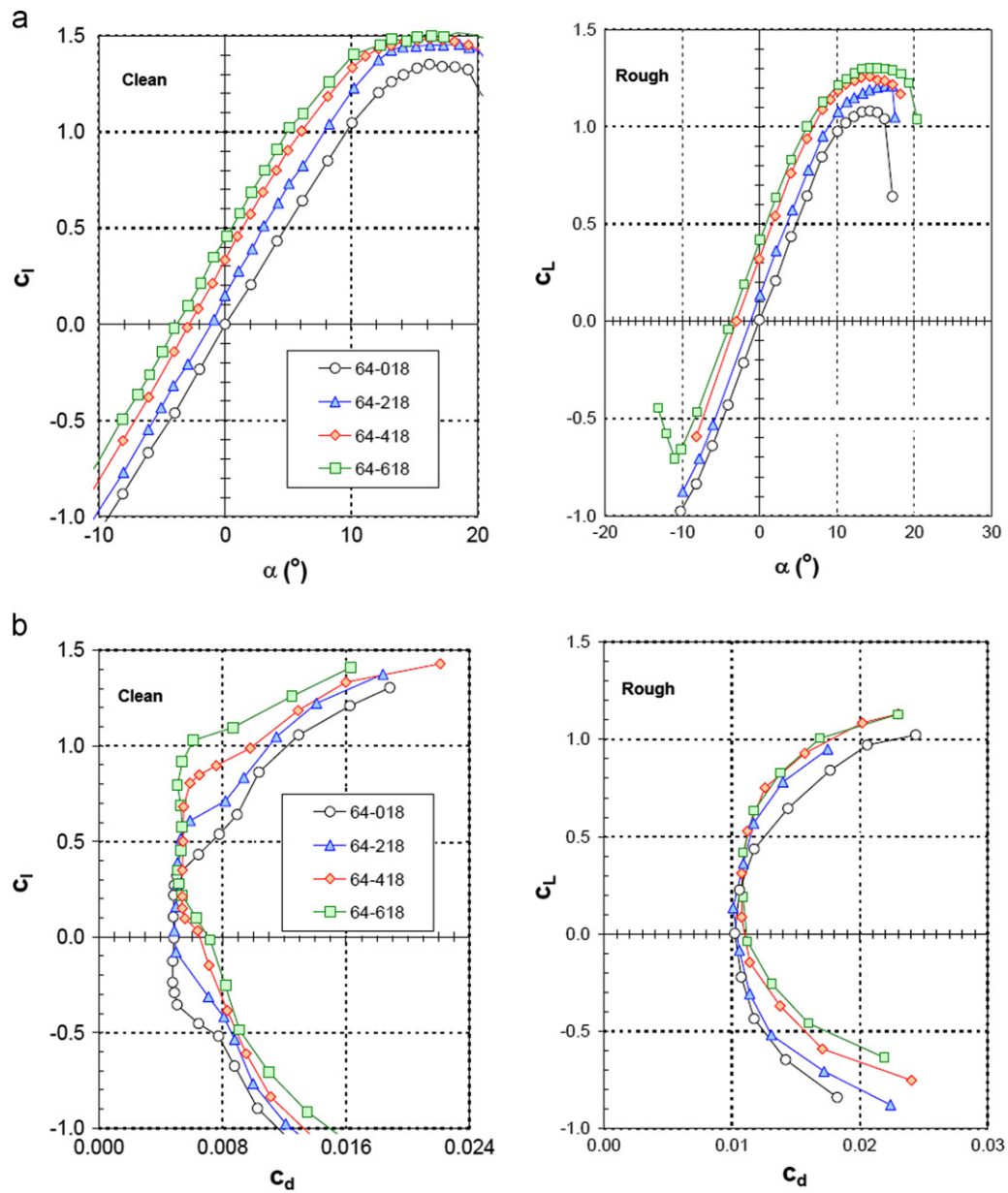


Fig. 11. (a) Lift coefficients of clean and rough members of the NACA 64-x18 airfoil family [17]; and (b) drag vs. lift coefficients of clean and rough members of the NACA 64-x18 airfoil family [17].

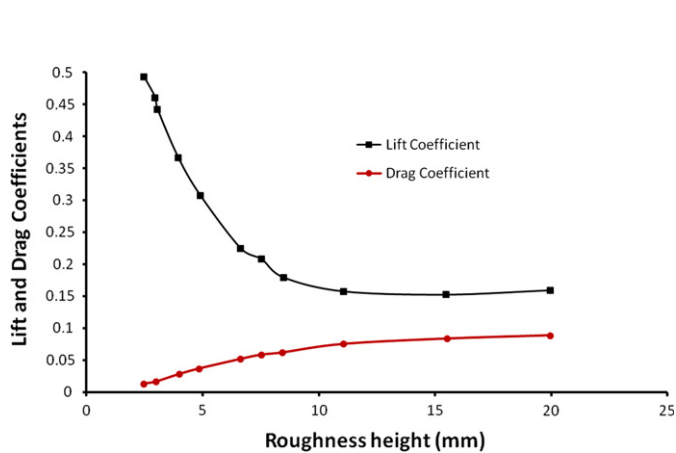


Fig. 12. Effect of roughness height on the lift and drag coefficients [18].

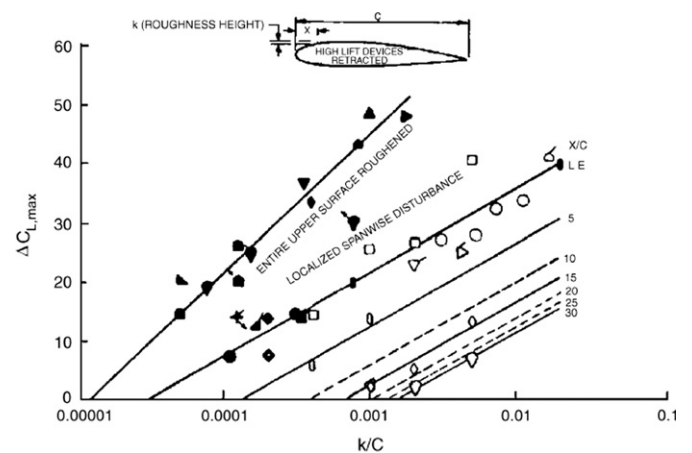


Fig. 13. Effect of roughness size and location on the lift coefficient [9].

the power curve of an operational wind turbine over time after a cleaning process was carried out. Fig. 15 shows that an increase in the operation time between surface cleanings decreases the power production of the turbine. However, at low wind speeds, power production is identical for both clean and contaminated wind turbine blades.

Another numerical simulation was performed by Ren and Ou [21] for continuous operational periods. The roughness height and the roughness area on a surface were estimated using empirical correlation, as proposed by Khalfallah [4]. Predicted lift and drag coefficients are presented in Fig. 16. Although the drag gradually increases, the lift coefficient shows a sudden reduction before the critical roughness height and the critical roughness area are reached.

5. Numerical efforts for modeling roughness

As the size of wind turbines grows, it is becoming more difficult and more expensive to perform full-scale experiments.

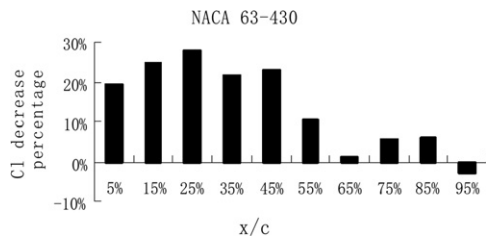


Fig. 14. Percentage of lift coefficient decrease for different roughness locations [21].

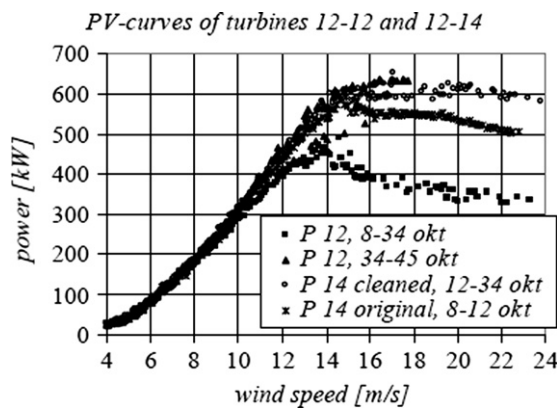


Fig. 15. Power production over varying operational times [5].

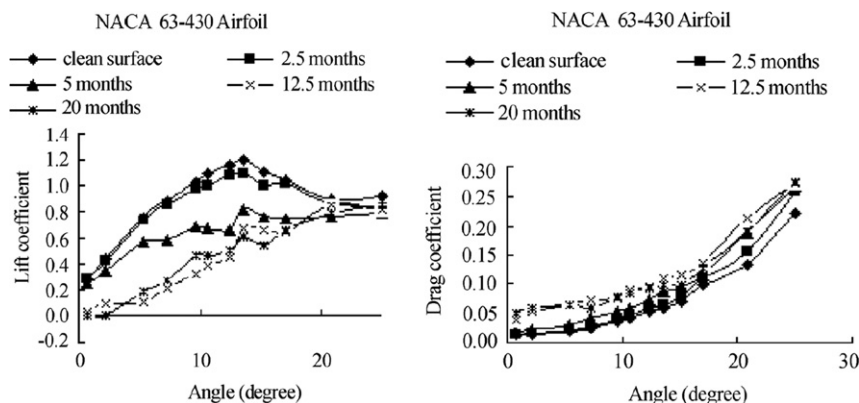


Fig. 16. Lift and drag curve estimation over varying operational periods [20].

Consequently, computational tools are preferred for the design and analysis of wind turbines. Several efforts [15,20–25] have been made to model roughness by modifying wall function terms in turbulence models. Turbulence modeling is an issue that has not yet been completely solved in flow field analysis, and different engineering applications may require different treatments of turbulence modeling for near wall flow. Consequently, modeling roughness where disturbances are created in that flow requires special attention. In the literature, there are some studies in which various turbulence models have been modified. Although not a recent one, a study by Patel and Yoon [22] gives a good review of the turbulence models available that are applied to rough surfaces. These authors concluded at the time that the best model was the $k-\omega$ model with Wilcox roughness modification.

Later, Durbin et al. [23] developed a prediction method for the $k-\epsilon$ turbulence model based on inserting a hydrodynamic roughness length into the model transport equations and modifying the boundary conditions of the turbulent kinetic energy equation. These roughness formulations have been validated against experimental data available in the literature. The comparison shows that rough wall boundary layer characteristics can be modeled accurately, except at the beginning of the separation, where there is an adverse pressure gradient. Nevertheless, prediction of this situation is difficult, even for smooth walls.

A more recent study has been conducted by Knopp et al. [24], who apply a roughness correction to the famous $k-\omega$ SST turbulence model. To quantify the characteristics of roughness, they also apply equivalent sand grain roughness to the model. This paper addresses two major shortcomings of the Wilcox roughness correction mentioned above. These are the requirement for a very fine grid resolution near the wall, which increases the computational cost significantly, and poor prediction of the skin friction coefficient. Moreover, the Wilcox roughness modification cannot be applied directly to the $k-\omega$ SST model, which is frequently used in aeronautical applications. As it is outside the scope of this paper, details on the turbulence model modification are not addressed here. Comparisons of the lift coefficient over the NACA 65-215 airfoil are presented for the roughness modified Spalart–Allmaras model and the $k-\omega$ SST model. As we can see in Fig. 17, the proposed new method predicts the lift coefficient quite well, compared to Spalart–Allmaras, which overshoots this coefficient at higher angles of attack, for both clean and rough configurations. This advancement is important, since numerical prediction of the maximum lift coefficient is still a problem.

Ferrer and Munduate [15] have performed numerical simulations on an S814 airfoil using the commercial CFD code ANSYS FLUENT 12.0.3 and panel code XFOIL 6.9. Transition is modeled using Menter–Langtry correlation, and fully turbulent flow is

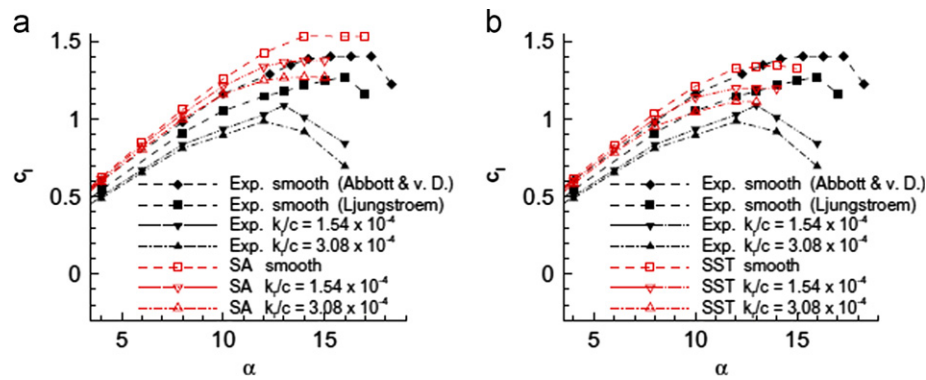


Fig. 17. Lift coefficient curve comparison: (a) Spalart–Allmaras model; and (b) $k-\omega$ SST model [24].

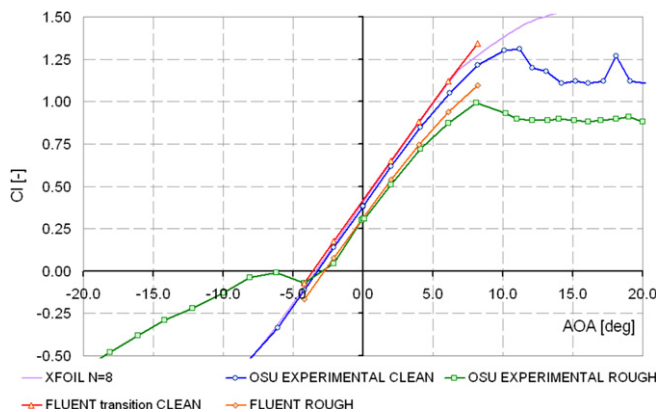


Fig. 18. Lift coefficient curve of an S814 airfoil from various analyses [15].

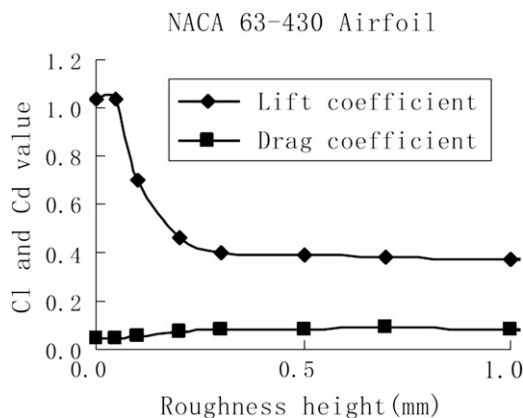


Fig. 19. Lift and drag coefficients for various roughness heights [20].

modeled using the $k-\omega$ SST turbulence model. For the rough configurations, flow is assumed to be fully turbulent. Comparisons of numerical simulations against experimental data show that the commercial code predicts lift coefficients well for both clean and rough surfaces, as shown in Fig. 18. However, for the rough case, the flow is assumed to be fully turbulent, and simulations at higher angles of attack have not yet yielded converging results. So, while current numerical schemes are capable of modeling roughness, they cannot do so at higher angles of attack.

In another study [20], a NACA 63430 airfoil that is used extensively in wind turbine applications is simulated for both smooth and rough configurations. Numerical simulations are performed assuming fully turbulent flow, in which the $k-\omega$ SST turbulence model is applied. Fig. 19 proves that roughness causes

a significant reduction in the lift coefficient and a slight increase in the drag coefficient. As expected, beyond a critical roughness height, the lift and drag coefficients become insensitive to this parameter.

A study by Villalpando et al. [25] has also proved the ability of the $k-\omega$ SST model on an iced NACA 63–415 airfoil for various Reynolds numbers and angles of attack.

6. Solutions to the roughness problem

Solutions to eliminate the effects of roughness can be categorized as either design solutions or external solutions. Design solutions include the use of airfoils that are specifically designed and optimized for both clean and rough configurations. External solutions, by contrast, include various applications that lessen the effect of roughness on wind turbine performance, like special coatings that decrease the number of water droplets that stick to the blade, deicing equipment, and manual cleaning of the blades.

6.1. Specially designed airfoils

The National Renewable Energy Laboratory (NREL), formerly the Solar Energy Research Institute, originated the design of airfoils specifically for wind turbines, as aircraft airfoils generate excessive power at high wind speeds, which results in generator burn-out, and they are very sensitive to surface roughness [26]. So, a variety of airfoils have been designed based on the differing design requirements of spanwise sections and blade sizes. These airfoil families have the following advantages:

- Lower maximum lift coefficient at the tip of the blade to control peak power and prevent generator burn-out;
- Higher maximum lift coefficient at the root location to improve start-up at low wind speeds;
- Less sensitivity to roughness effects by forcing laminar to turbulent transition on both the upper and lower surfaces as maximum lift coefficient is reached.

In Fig. 20, the power production of SERI blades, which are specially designed airfoils, and AEROSTAR blades, which are aircraft airfoils for clean and contaminated configurations, are compared. The maximum power production of a SERI blade is limited to 65 kW to prevent generator burn-out. The power production of a dirty SERI blade is markedly better than that of the AEROSTAR blade. The corresponding Annual Energy Production (AEP) is also much improved, with a 10% improvement for the clean blade and a 30% improvement for the contaminated blade.

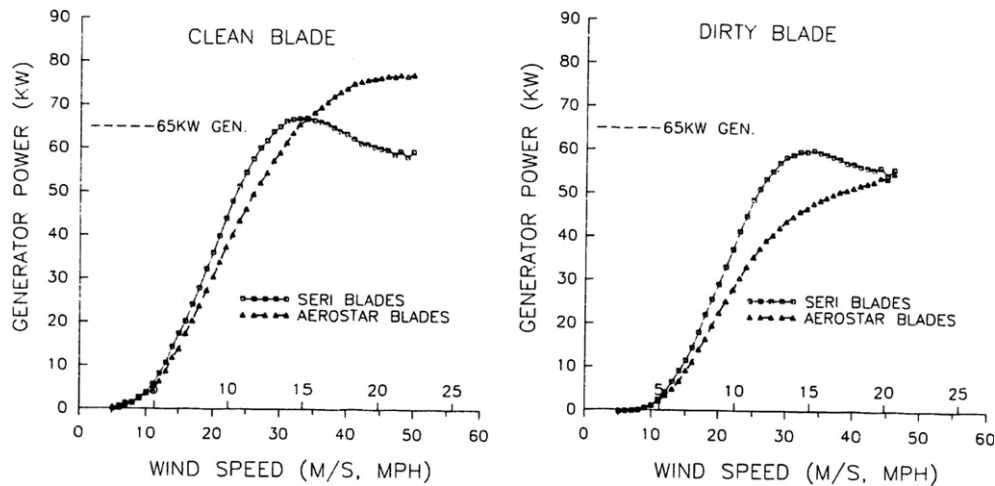


Fig. 20. Comparison of wind turbine airfoils for clean and dirty configurations [26].

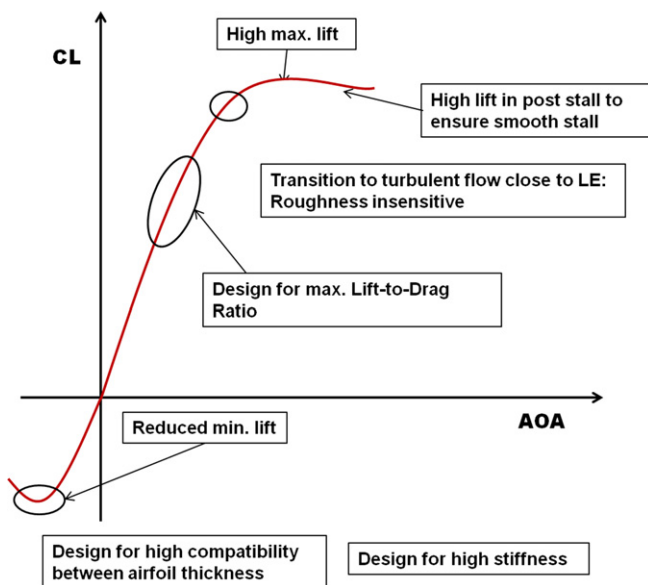


Fig. 21. Design requirements and objectives for design optimization on the lift coefficient curve [28].

Bak [27,28] also conducted a study to search for a wind turbine airfoil family that is insensitive to roughness and turbulence intensity. In this case, the airfoil geometry was optimized for both the clean and rough configurations by means of a generic quasi 3D multidisciplinary optimization tool, while at the same time maintaining high aerodynamic efficiency and stiffness. The design variable for this optimization is the airfoil shape, and the design objective is the maximum lift-to-drag ratio. The design optimization strategy is schematized in Fig. 21. The optimization is performed at two locations on the rotor, and the thickness of rest of the blade is obtained through interpolation.

The wind tunnel test results of these airfoils show that the maximum lift coefficient decreases only slightly when roughness is introduced. However, the difference between the clean and rough configurations is more noticeable in the lift/drag ratio comparison. This difference is due to the fact that the behavior of the drag coefficient, unlike that of the lift coefficient, is rather sensitive.

Rooij and Timmer [29] review the performance of 25–30% thick wind turbine airfoils with an emphasis on roughness sensitivity. Wind tunnel data were derived from the literature,

and rotational effects were introduced using the RFOIL code, which predicts aerodynamic performance, including rotational effects. The wind tunnel results for clean and rough configurations are compared in Fig. 22(a) and (b), respectively, for the DU 91-W2-250, S814, and NACA 63-425 airfoils. As we can see, while the maximum lift coefficient of the NACA airfoil decreases significantly, the lift reduction for the other airfoils is more acceptable. These results are expected, however, as the NACA airfoil was not specifically designed for wind turbine applications. The lift-to-drag ratio decreases for all airfoils, as the drag remains sensitive to the roughness elements. However, this reduction is even more remarkable for the NACA airfoil.

6.2. External solutions

Vortex generators, surface finishes or coatings, and cleaning are the best known and most widely used solutions for moderating the effects of roughness.

Vortex generators located on blades improve flow quality and airfoil performance by preventing separation and increasing lift. Rooij and Timmer [29] review the wind turbine airfoils equipped with vortex generators, and their results are presented in Table 2. The application of vortex generators reduces roughness sensitivity, further increasing the maximum lift coefficient of the airfoil.

Surface finishing paints are designed to improve surface quality and extend the lifetime of blades by preventing cracks; however, a painted surface still has some roughness, depending on the type of finish applied. As indicated in Table 1, spray painting results in better quality in the absence of any roughness elements in the application environment. Moreover, as Parent and Ilinca [30] show in their review, nonstick coating applications are being developed for wind turbines. For an icy environment, this application may prevent the build-up of ice particles, and consequently prevent surface roughness. There are other coatings available commercially that ensure minimum dirt build-up [31].

Besides these applications, Lachmann [7] proposes covering the surface with plastic films, scrapers, or similar materials, applying continuous liquid flow that will remove the contamination on the surface, and implementing boundary layer control to remove the turbulent boundary layer behind the roughened area.

If none of these solutions is applied, there is one ultimate, and basic, solution that is always available, which is manual cleaning of the blades. There are commercial companies that optimize the time required for blade cleaning, as a function of the wind turbine and wind farm characteristics [32,33].

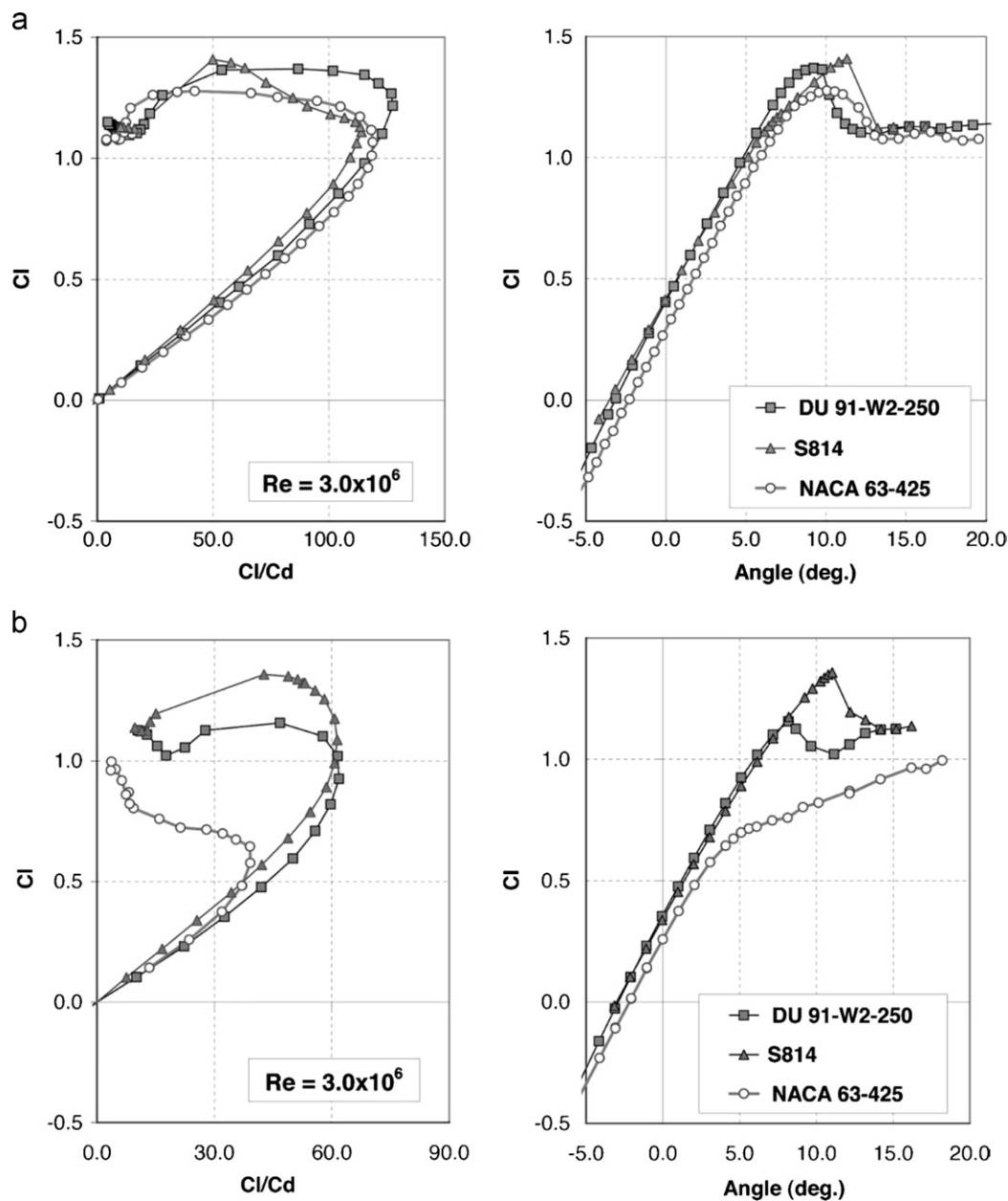


Fig. 22. Lift coefficient and lift-to-drag ratio for: (a) clean; and (b) rough configurations [29].

Table 2

Comparison of wind turbine airfoils with vortex generators [29].

| Configuration | | Clean | | "Rough" | |
|-----------------------------|--------------------------------|---------|--------|---------|--------|
| Airfoil | Position VG (α/c) (%) | L/D-max | Cl-max | L/D-max | Cl-max |
| $Re = 2.0 \times 10^6$ | | | | | |
| DU 91-W2-250 ⁽¹⁾ | 20 | 66.4 | 1.9 | | |
| DU 91-W2-250 ⁽¹⁾ | 30 | 73.9 | 1.89 | | |
| DU 97-W-300 ⁽²⁾ | 20 | 63.2 | 1.97 | 53.2 | 1.93 |
| | 30 | 69.1 | 1.88 | | |
| $Re = 1.6 \times 10^6$ | | | | | |
| Risø-A1-24 ⁽⁴⁾ | 20 | 47.1 | 1.805 | 41.9 | 1.77 |
| FFA-W3-241 ⁽⁴⁾ | 20 | 45.6 | 1.543 | 44.4 | 1.38 |
| FFA-W3-241 ⁽⁴⁾ | 30 | 59.1 | 1.54 | 51.6 | 1.43 |
| FFA-W3-301 ⁽³⁾ | 20 | 38.7 | 1.636 | | |
| FFA-W3-301 ⁽³⁾ | 30 | 39.2 | 1.36 | 32.2 | 1.02 |
| NACA 63-430 ⁽³⁾ | 20 | 31.9 | 1.3 | | |
| NACA 63-430 ⁽³⁾ | 30 | 45.6 | 1.37 | 36.5 | 1.13 |

7. Concluding remarks

- Contamination agents like dust, ice, and insects decrease the performance of wind turbines.
- The presence of roughness elements provokes early transition and increases the extent of transitional flow, as well as increasing turbulence intensity near the wall.
- For numerical modeling and wind tunnel experiments, contamination patterns can be replaced by an equivalent sand grain roughness. This eliminates the need for 3D molds in wind tunnel experiments.
- Roughness size, density, and location are the most important parameters influencing wind turbine performance, which tends to decrease with increasing roughness size and density. However, there is a level of roughness height after which the performance remains stable, which is called the critical roughness size. In terms of roughness distribution, the leading edge is the location that is the most sensitive to roughness

elements, while trailing edge roughness has almost no effect on performance.

- There is a limit to the Reynolds number under which the performance is not affected.
- Although numerical models are capable of predicting clean wind turbine performance, the accurate simulation of rough configurations is still under development. Currently, $k-\omega$ SST seems to be the most accurate turbulence model.
- To lessen or even eliminate the effects of roughness on performance, specially designed airfoils are found to be the best and most widely used solution. When roughness sensitivity is regarded as a design parameter, the resulting airfoils are significantly less influenced by roughness.

References

- [1] Weiss P. Insects in the wind lead to less power. Retrieved from http://www.sciencenews.org/view/generic/id/1854/description/Insects_in_the_wind_lead_to_less_power in November 2012.
- [2] Wind turbine ice protection system. Retrieved from http://www.kellyaerospace.com/wind_turbine_deice.html in November 2012.
- [3] Blade Smart. General description of Gurney flaps. Retrieved from in <http://smart-blade.com/products-services/gurney-flaps.html> in November 2012.
- [4] Khalfallah MG, Koliub AM. Effect of dust on the performance of wind turbines. *Desalination* 2007;209:209–20.
- [5] Corten GP, Veldkamp HF. Insects cause double stall. Copenhagen: EWEC; 2001.
- [6] Corten GP, Veldkamp HF. Insects can halve wind-turbine power. *Nature* 2001;412:41.
- [7] Lachmann GR. Aspects of insect contamination in relation to laminar flow aircraft. Aeronautical Research Center Technical report C. P. no. 484.
- [8] Petrone G, de Nicola C, Quagliarella D, Witteveen J, Iaccarino G. Wind turbine performance analysis under uncertainty. In: 49th AIAA aerospace sciences meeting including the new horizons forum and aerospace exposition. January 4–7, Orlando, FL: USA; 2011.
- [9] Bragg MB, Broeren AP, Blumenthal LA. Iced airfoil aerodynamics. *Progress in Aerospace Sciences* 2005;41:323–62.
- [10] Pechlivanoglou G. The effect of distributed roughness on the power performance of wind turbines. *ASME Turbo Expo* 2010;5:845–55.
- [11] Schlichting H. Boundary layer theory. 7th ed. McGraw Hill Book Company; 1979 (Original Work Published in 1951).
- [12] Busch G. Experimental study of full scale iced-airfoil aerodynamic performance using subscale simulations. PhD dissertation. University of Illinois at Urbana-Champaign; 2009.
- [13] Turner AB, Hubbe-Walker SE, Bayley FJ. Fluid flow and heat transfer over straight and curved rough surfaces. *International Journal of Heat and Mass Transfer* 2000;43:251–62.
- [14] Kerho M, Bragg MB. Airfoil boundary-layer development and transition with large leading-edge roughness. *AIAA Journal* 1997;35(1).
- [15] Ferrer E, Munduate X. CFD predictions of transition and distributed roughness over a wind turbine airfoil. In: 47th AIAA aerospace sciences meeting. January; 2009.
- [16] Freudenreich K, Kalser K, Schaffarczyk A P, Winkler H, Stahl B. Reynolds number and roughness effects on thick airfoils for wind turbines. *Wind Engineering* 2004;28(5):529–46.
- [17] Timmer, WA. An overview of NACA 6-digit airfoil series characteristics with reference to airfoils for large wind turbine blades. In: AIAA 2009-268. 47th AIAA aerospace sciences meeting including the new horizons forum and aerospace exposition. January 5–8, Orlando, FL; USA; 2009.
- [18] Li, D, Li, R, Yang, C, Wang, X. Effects of roughness on aerodynamics performance of a wind turbine airfoil. 2010.
- [19] Gregory N, O'Reilly L. Low speed aerodynamic characteristics of NACA 0012 aerofoil section, including the effects of upper-surface roughness simulating hoar frost. Aeronautical Research Council reports and memoranda. London; UK; 1973.
- [20] Ren N, Ou J. Numerical simulation of surface roughness effect on wind turbine thick airfoils. 2009 Asia-Pacific power and energy engineering conference, p. 4. 2009.
- [21] Ren N, Ou J. Dust effect on the performance of wind turbine airfoils. *Journal of Electromagnetic Analysis and Applications* 2009;1(2):102–7.
- [22] Patel VC, Yoon JY. Application of turbulence models to separated flow over rough surfaces. *Journal of Fluids Engineering* 1995;117(2):234.
- [23] Durbin PA, Medic G, Seo JM, Eaton JK, Song S. Rough wall modification of two layer $k-\epsilon$ model.
- [24] Knopp T, Eisfeld B, Calvo JB. A new extension for $k-w$ turbulence model to account for wall roughness. *International Journal of Heat and Fluid Flow* 2009;30:54–65.
- [25] Villalpando F, Reggio M, Ilinca A. Numerical study of flow around iced wind turbine airfoil. *Engineering Applications of Computational Fluid Mechanics* 2012;6(1):39–45.
- [26] Tangler J, Smith B, Jager D. SERI advanced wind turbine blades. National Renewable Energy Laboratory NREL-TP-257-4492. February; 1992.
- [27] Bak C. Design and verification of airfoils resistant to surface contamination and turbulence intensity. In: 26th AIAA applied aerodynamics conference. August; 2008.
- [28] Fuglsang P, Bak C, Gaunaa M, Antoniou I. Design and verification of the Riso-B1 airfoil family for wind turbines. *Journal of Solar Energy Engineering, Transactions of the ASME* 2004;126(4):1002–10 Wind Energy.
- [29] van Rooij RPJOM, Timmer WA. Roughness sensitivity considerations for thick rotor blade airfoils, vol. 125. ASME; 2003.
- [30] Parent O, Ilinca A. Anti-icing and de-icing techniques for wind turbines: critical review. *Cold Regions Science and Technology* 2011;65(1):88–96.
- [31] BladeSkyn technical data sheet. Retrieved from www.bladedynamics.com in April; 2012.
- [32] Blade access cleaning system for wind turbines. Retrieved from www.ismhelp.com in April; 2012.
- [33] BladeCleaning Limpieza de Palas. from www.bladecleaning.com in April; 2012.